State-of-Charge Estimation for Lithium-Ion Batteries Using Neural Networks and EKF

Mohammad Charkhgard and Mohammad Farrokhi, *Member, IEEE*

***Abstract*—This paper presents a method for modeling and estimation of the state of charge (SOC) of lithium-ion (Li-Ion) batteries using neural networks (NNs) and the extended Kalman filter (EKF). The NN is trained offline using the data collected from the battery-charging process. This network finds the model needed in the state-space equations of the EKF, where the state variables are the battery terminal voltage at the previous sample and the SOC at the present sample. Furthermore, the covariance matrix for the process noise in the EKF is estimated adaptively. The proposed method is implemented on a Li-Ion battery to estimate online the actual SOC of the battery. Experimental results show a good estimation of the SOC and fast convergence of the EKF state variables.**

***Index Terms*—Batteries, estimation, Kalman filtering, monitoring, neural networks (NNs).**

I. Introduction

SOME batteries are sensitive to overcharge and/or deep discharge, which may lead to permanent damages to these devices [1], [2]. In the charging process, it is usually desirable to charge the battery with the highest and the safest current in order to reach the full state of charge (SOC) as quickly as possible without entering the overcharge region [1], [3]. Therefore, it is necessary to measure the SOC with good accuracy for proper battery management [2], [4]–[7]. Moreover, the state of health (SOH) of batteries requires maintaining the SOC continuously within certain limits [2], [3], [8].

The SOC definition, in the simplest way, is the ratio between the saved energy in the battery and the whole energy that can be saved in it [2], [3]. The SOC estimation is not an easy task and depends on the battery type and applications [2]. Generally, there are two categories for the SOC estimation: indirect and direct methods. In indirect methods, the SOC is estimated from some physical properties of the battery, such as the acid density or cathodic galvanostatic pulses. Estimating these quantities needs precise measurements and has several limitations in practice [3], [9]. One of the indirect methods is measuring the open-circuit voltage of the battery. In this method, the battery must be relaxed for some time to allow its open-circuit voltage to reach a steady-state condition. Therefore, this method is not practical in applications where the battery is not allowed to be opened from the electric circuit [2], [3], [10]. In other methods, the SOC is estimated using the discharge voltage of the battery [11], [12]. In [12], only the remaining time to reach the end-of-discharge voltage of the battery is estimated using artificial neural networks (ANNs). Impedance spectroscopy is a commonly used indirect method for electrochemical processes such as batteries. This method is used not only for the SOC estimation but also for the SOH estimation [13], [14]. However, this approach requires some additional measurements that make it suitable in laboratory tests, but not in practical applications [2], [3]. In [15], the battery impedance is measured directly through frequency variations to improve the charging process. In [16], the SOC is determined using the voltage of the estimated electromotive force. In this paper, it is necessary to measure the battery impedance with ac current and voltage, which seems to be suitable for laboratory tests. Some researchers have used fuzzy logic to model the relationship between the battery SOC and its parameters based on impedance spectroscopy measurements [17], [18].

Among the direct methods for SOC estimation is the ampere–hour counting technique. This method needs the initial SOC, calculation of the internal consumptions of the battery, and accurate current sensors [2], [19]. ANNs have also been used by some researchers for direct estimation of the SOC [20]–[28]. In these methods, there is a need for some input–output data as the training set, which must be obtained by some other estimation methods. The trained network can then be used to estimate the SOC.

The Kalman filter (KF) is a powerful tool for the state estimation of systems. Some researchers have used this filter to estimate the open-circuit voltage or other parameters of batteries that have a direct relationship with the SOC [29]–[32]. In [33] and [34], the KF is employed to estimate some physical quantities, which have direct effects on the SOC. In some papers, the SOC is defined as a model state and is estimated using the KF [8], [35]–[37]. However, the KF needs a suitable model of the battery. Moreover, due to the use of feedbacks in this filter, there is a need for proper initialization of states; otherwise, its states may not converge.

In this paper, a state-space model of the SOC is proposed that is approximated using a neural network (NN). Then, by using this model and the extended KF (EKF), the battery SOC is estimated. The proposed method is implemented and tested on a lithium-ion (Li-Ion) battery. The experimental results show good accuracy and quick convergence for estimating the SOC of Li-Ion batteries.

Manuscript received September 19, 2008; revised February 7, 2009, July 10, 2009, and September 29, 2009; accepted December 16, 2009. Date of publication February 18, 2010; date of current version November 10, 2010.

M. Charkhgard is with the Department of Electrical Engineering, Iran University of Science and Technology, Tehran 16846, Iran.

M. Farrokhi is with the Department of Electrical Engineering and the Center of Excellence for Power System Automation and Operation, Iran University of Science and Technology, Tehran 16846, Iran (e-mail: farrokhi@iust.ac.ir).

Color versions of one or more of the figures in this paper are available online at http://ieeexplore.ieee.org.

Digital Object Identifier 10.1109/TIE.2010.2043035

This paper is organized as follows. Section II describes the battery model. Section III presents the proposed SOC estimation algorithm. Section IV shows the experimental setups and results. Finally, Section V draws some conclusions and gives directions for the future work.

II. Modeling

In this paper, the SOC is defined as an independent state-space variable and is modeled using radial basis function (RBF) NNs [38].

A. SOC as State-Space Variable

The SOC can be defined as the ratio between the saved energy in a battery and the whole energy that could be saved in it [3], [16], [35]

$$z(t) = z(t_0) + \int_{t_0}^{t} \frac{\eta_i \, i(\tau)}{C_n} \, d\tau \tag{1}$$

where $z(t)$ is the SOC, $z(t_0)$ is the initial SOC, C_n is the nominal capacity, $i(t)$ is the instantaneous current (positive for discharge and negative for charge), and η_i is the Coulombic efficiency ($\eta_i = 1$ for discharge and $\eta_i = \eta \leq 1$ for charge) [35].

In order to employ the KF, it is necessary to discretize the model in (1). Assuming that the sampling rate Δt is small enough and substituting the integral with the Euler approximation, (1) can be written as

$$z(k+1) = z(k) + \frac{\eta_i \, \Delta t}{C_n} i(k). \tag{2}$$

As shown in (2), the SOC is defined as an independent state variable in the state-space model. Other state variables and the output equation will be given in the next section.

B. Proposed Model

The SOC of batteries has a nonlinear relationship with its terminal voltage and current [32]. It is usually not an easy task to obtain this nonlinear relationship. One way to find this relationship is to analyze the chemical reaction equations, which is very complicated.

In some papers, researchers propose the electrical model of batteries using resistances, capacitances, and inductances. The inductances are due to the geometry of electrodes and connectors. In many applications, the effect of inductances is neglected due to their small values [15], [33]. As a result, the battery model is reduced to an RC model, where the governing differential equation between the voltage and current is of the first order [16], [30], [31]. Therefore, in the discrete model, it is reasonable to consider the battery terminal voltage at the sampling time k as a nonlinear function of the voltage at the sampling time $(k-1)$ and the current and the SOC at the sampling time k [36].

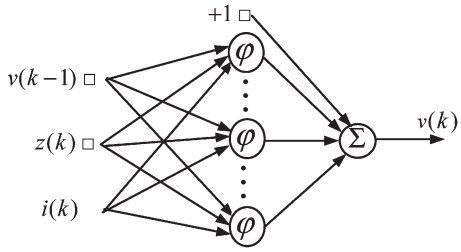

Fig. 1. Structure of the RBF NN for modeling.

Fortunately, ANNs are universal approximators and can approximate any nonlinear function with desired accuracies [38]. In this paper, RBF NNs are used to find the nonlinear model. Fig. 1 shows the structure of an RBF NN, where the inputs are the battery voltage at the sampling time $(k-1)$, the estimated SOC at the sampling time k, and the battery terminal current at the sampling time k. The NN finds an approximation of the battery terminal voltage at the sampling time k. The activation functions of neurons in the hidden layer are Green functions (e.g., Gaussian functions) in the following form:

$$\varphi_i(\mathbf{r}_k) = G\left(\|\mathbf{r}_k - \mathbf{t}_i\|\right) = \exp\left(-\frac{\|\mathbf{r}_k - \mathbf{t}_i\|^2}{\sigma_i^2}\right), \quad i = 1, \ldots, M \tag{3}$$

where $\mathbf{r}_k = [\, v(k-1) \quad z(k) \quad i(k) \,]^{\mathrm{T}}$ is the input vector applied to the network at the sampling time k, $\mathbf{t}_i$ and σ_i are the center and the standard deviation of the Gaussian function, respectively, and M is the number of neurons in the hidden layer. In fact, the output of this NN (i.e., the battery terminal voltage at the sampling time k) is the sum of the weighted Gaussian functions as

$$F(\mathbf{r}_k) = w_0 + \sum_{i=1}^{M} w_i \varphi_i\left(\|\mathbf{r}_k - \mathbf{t}_i\|\right) \tag{4}$$

where w_i $(i = 1, \ldots, M)$ is the weight vector connecting the ith neuron in the hidden layer to the output layer and w_0 is the bias weight for the linear output neuron. The free parameters of this network are $\mathbf{t}_i$, σ_i, w_i, and w_0. These parameters are defined during the training phase of the network using algorithms such as the back-propagation and the least mean square algorithms [38]. It should be noted that all inputs and the output variables of the NN are normalized.

Considering the battery terminal voltage at the sampling time $(k-1)$ and the SOC at k as the first and the second state variables, respectively, the state vector is defined as

$$\mathbf{x}_k := \begin{bmatrix} x_1(k) \\ x_2(k) \end{bmatrix} = \begin{bmatrix} v(k-1) \\ z(k) \end{bmatrix}$$

$$\Rightarrow \quad \mathbf{x}_{k+1} = \begin{bmatrix} x_1(k+1) \\ x_2(k+1) \end{bmatrix} = \begin{bmatrix} v(k) \\ z(k+1) \end{bmatrix} \tag{5}$$

where v and z represent the terminal voltage and the SOC of the battery, respectively. By using the aforementioned definition,

the state-space model can be defined in the following form:

$$\begin{bmatrix} x_1(k+1) \\ x_2(k+1) \end{bmatrix} = \begin{bmatrix} F(\mathbf{r}_k) \\ x_2(k) + \frac{\eta_i \Delta t}{C_n} i_k \end{bmatrix} + \begin{bmatrix} \omega_1(k) \\ \omega_2(k) \end{bmatrix}$$
$$\begin{bmatrix} y_1(k) \\ y_2(k) \end{bmatrix} = \begin{bmatrix} F(\mathbf{r}_k) \\ x_1(k) \end{bmatrix} + \begin{bmatrix} \upsilon_1(k) \\ \upsilon_2(k) \end{bmatrix} \tag{6}$$

where $F(\mathbf{r}_k)$ is the nonlinear function, which will be approximated by the RBF network and vectors $\boldsymbol{\omega} = [\omega_1 \quad \omega_2]^{\mathrm{T}}$ and $\boldsymbol{\upsilon} = [\upsilon_1 \quad \upsilon_2]^{\mathrm{T}}$ are the process and the measurement noises, respectively, with covariance matrices

$$\mathbf{Q}_k := E[\boldsymbol{\omega}_k \quad \boldsymbol{\omega}_k^{\mathrm{T}}] \quad \mathbf{R}_k := E[\boldsymbol{\upsilon}_k \quad \boldsymbol{\upsilon}_k^{\mathrm{T}}]. \tag{7}$$

Moreover, $\mathbf{r}_k$ (i.e., the normalized input vector to the NN) is defined as

$$\mathbf{r}_k := [\mathbf{x}_k^{\mathrm{T}} \quad i_k]^{\mathrm{T}} \tag{8}$$

where $\mathbf{x}_k$ is given in (5). Notice that the battery terminal voltages at k and $(k-1)$ [i.e., the output variables $y_1(k)$ and $y_2(k)$] are used in the proposed model.

III. Estimation Algorithm

The estimation algorithm, in this paper, is based on the EKF. The performance of KF depends on several factors, e.g., the dependence on an accurate state-space model of the system that was proposed in the previous section.

A. Adaptive EKF

The KF that is estimating the states of a linear time-varying model, which approximates the nonlinear model, is called the EKF. Hence, if the system has a nonlinear model, the nonlinear system must be linearized around the operating point with a time-varying approximation. Even though the performance of EKF is not optimal, it works fine for most applications [39]. One important issue in designing a KF is the proper selection of covariance matrices for the measurement and process noises. The covariance matrix of the measurement noise $(\mathbf{R})$ can be determined directly from the battery data. The variances can be obtained from the square of the root mean square (rms) of noisy measurements of the battery terminal voltage. It is assumed that the variances are independent and have Gaussian distributions [30]. The covariance matrix of the process noise $(\mathbf{Q})$ is estimated in this paper using the Maybeck's estimator as [40]

$$\hat{\mathbf{Q}}_k = \frac{1}{N} \sum_{j=k-N+1}^{k} \left[\mathbf{G}_j \mathbf{v}_j \mathbf{v}_j^{\mathrm{T}} \mathbf{G}_j^{\mathrm{T}} - \left(\mathbf{A}_{j-1} \mathbf{P}_{j-1} \mathbf{A}_{j-1}^{\mathrm{T}} \mathbf{P}_{j-1} \right) \right] \tag{9}$$

where matrices $\mathbf{G}$, $\mathbf{A}$, and $\mathbf{P}$ are given in Table I, N is the number of recent sample periods, and $\boldsymbol{\nu}$ is the innovation vector calculated as

$$\boldsymbol{\nu}_j = \mathbf{y}_j - \mathbf{h}\left(\hat{\boldsymbol{x}}_j^-, \mathbf{u}_j\right). \tag{10}$$

Some clarification about the adaptive algorithm, given in (9), is in order here. The fundamental of the adaptive KF (i.e., KF with adaptive covariance matrix) is based on "whitening" of the innovation sequence ("white" refers to the white stochastic process). Whitening the innovation process means that $E[\boldsymbol{\nu}_k \quad \boldsymbol{\nu}_{k-j}^{\mathrm{T}}]$ should be positive semidefinite for $j = 0$ and zero for $j > 0$. Kailath [41] has pointed out that the adaptive algorithm for KF guarantees optimality but does not guarantee the calculated covariance to be true. Myers and Tapley [42] also showed that their adaptive filter resulted in negative definite covariance for the process noise. To solve this problem, they reset all the diagonal elements to their absolute value. Blanchet *et al.* [43] have employed a different approach. They calculate eigenvalues of $\mathbf{Q}$ in each time step and substitute the negative eigenvalues with zero. The latter approach is used in this paper, i.e., negative eigenvalues of the calculated matrix $\mathbf{Q}$ in the adaptive filter are set to zero.

For convenience, a summary of the employed adaptive EKF algorithm is given in Table I.

TABLE I
Summary of Adaptive EKF Algorithm

State space model

$$\mathbf{x}_{k+1} = \mathbf{f}(\mathbf{x}_k, \mathbf{u}_k) + \boldsymbol{\omega}_k$$
$$\mathbf{y}_k = \mathbf{h}(\mathbf{x}_k, \mathbf{u}_k) + \mathbf{v}_k$$

where $\boldsymbol{\omega}_k$ and $\mathbf{v}_k$ are independent, zero mean, Gaussian process and measurement noises with covariance matrices $\mathbf{Q}_k = E[\boldsymbol{\omega}_k \boldsymbol{\omega}_k^T]$ and $\mathbf{R}_k = E[\mathbf{v}_k \mathbf{v}_k^T]$, respectively

Definition

$$\mathbf{A}_k = \left.\frac{\partial \mathbf{f}(\mathbf{x}_k, \mathbf{u}_k)}{\partial \mathbf{x}}\right|_{\mathbf{x}=\hat{\mathbf{x}}_k}, \quad \mathbf{C}_k = \left.\frac{\partial \mathbf{h}(\mathbf{x}_k, \mathbf{u}_k)}{\partial \mathbf{x}}\right|_{\mathbf{x}=\hat{\mathbf{x}}_k^-}$$

Initialization

$$\hat{\mathbf{x}}_0 = E[\mathbf{x}_0],$$
$$\mathbf{P}_0 = E\left[(\mathbf{x}_0 - E[\mathbf{x}_0])(\mathbf{x}_0 - E[\mathbf{x}_0])^T\right]$$

Calculating for $k = 1, 2, \ldots$

Time update

State estimate propagation

$$\hat{\mathbf{x}}_k^- = \mathbf{f}(\hat{\mathbf{x}}_{k-1}, \mathbf{u}_{k-1})$$

Error covariance propagation

$$\mathbf{P}_k^- = \mathbf{A}_{k-1} \mathbf{P}_{k-1} \mathbf{A}_{k-1}^T + \hat{\mathbf{Q}}_{k-1}$$

Measurement update

Kalman gain matrix

$$\mathbf{G}_k = \mathbf{P}_k^- \mathbf{C}_k^T (\mathbf{C}_k \mathbf{P}_k^- \mathbf{C}_k^T + \mathbf{R}_k)^{-1}$$

State estimate update

$$\mathbf{v}_k = \mathbf{y}_k - \mathbf{h}(\hat{\mathbf{x}}_k^-, \mathbf{u}_k), \quad \hat{\mathbf{x}}_k = \hat{\mathbf{x}}_k^- + \mathbf{G}_k \mathbf{v}_k$$

Error covariance update

$$\mathbf{P}_k = (\mathbf{I} - \mathbf{G}_k \mathbf{C}_k) \mathbf{P}_k^-$$

$$\hat{\mathbf{Q}}_k = \frac{1}{N} \sum_{j=k-N+1}^{k} \left[\mathbf{G}_j \mathbf{v}_j \mathbf{v}_j^T \mathbf{G}_j^T - \left(\mathbf{A}_{j-1} \mathbf{P}_{j-1} \mathbf{A}_{j-1}^T - \mathbf{P}_j \right) \right]$$

B. Linearization of the Proposed Model

In order to apply the EKF to the proposed nonlinear model in (6), the battery model must be linearized at every sampling instance. Define the nonlinear transition matrix function $\mathbf{f}(\mathbf{x}_k, \mathbf{u}_k)$ and the nonlinear measurement matrix $\mathbf{h}(\mathbf{x}_k, \mathbf{u}_k)$ as

$$\mathbf{f}(\mathbf{x}_k, \mathbf{u}_k) := \begin{bmatrix} F(\mathbf{r}_k) \\ x_2(k) + \frac{\eta_i \Delta t}{C_n} i_k \end{bmatrix} \quad \mathbf{h}(\mathbf{x}_k, \mathbf{u}_k) := \begin{bmatrix} F(\mathbf{r}_k) \\ x_1(k) \end{bmatrix}. \tag{11}$$

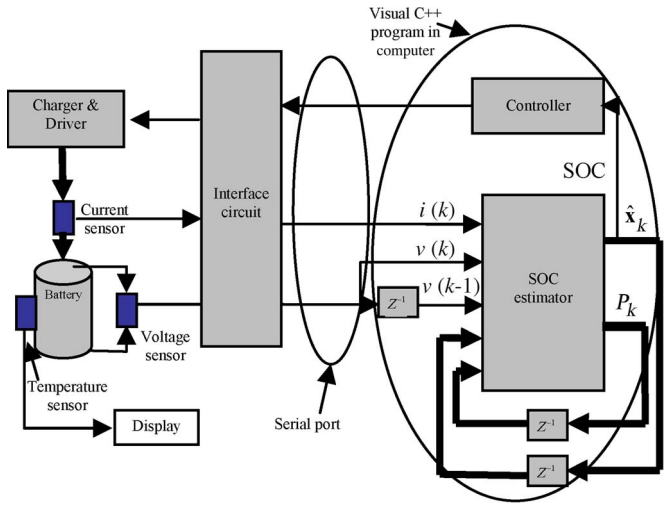

Fig. 2. General structure of the proposed system.

Differentiating $\mathbf{f}(\mathbf{x}_k, \mathbf{u}_k)$ and $\mathbf{h}(\mathbf{x}_k, \mathbf{u}_k)$ with respect to $\mathbf{x}_k$ and then letting $\mathbf{x}_k = \hat{\mathbf{x}}_k$ and $\mathbf{x}_k = \hat{\mathbf{x}}_k^-$, respectively, yield

$$\mathbf{A}_k = \left(\begin{matrix} \frac{\partial F(\mathbf{r}_k)}{\partial \mathbf{x}_k} \\ 0 \quad 1 \end{matrix} \right)_{\mathbf{x}_k = \hat{\mathbf{x}}_k} \qquad \mathbf{C}_k = \left(\begin{matrix} \frac{\partial F(\mathbf{r}_k)}{\partial \mathbf{x}_k} \\ 1 \quad 0 \end{matrix} \right)_{\mathbf{x}_k = \hat{\mathbf{x}}_k^-} \tag{12}$$

where $F(\mathbf{r}_k)$ is the output equation of the RBF NN. Hence

$$\frac{\partial F(\mathbf{r}_k)}{\partial \mathbf{x}_k} = \sum_{i=1}^{M} w_i \frac{\partial \varphi\left(\|\mathbf{r}_k - \mathbf{t}_i\|\right)}{\partial \mathbf{x}_k} \tag{13}$$

in which the derivative of $\varphi(\|\mathbf{r}_k - \mathbf{t}_i\|)$ with respect to $\mathbf{x}_k$ can be found using (3) as

$$\frac{\partial \varphi\left(\|\mathbf{r}_k - \mathbf{t}_i\|\right)}{\partial \mathbf{x}_k} = \left(\frac{\partial \varphi\left(\|\mathbf{r}_k - \mathbf{t}_i\|\right)}{\partial \mathbf{r}_k} \right)^{\mathrm{T}} \frac{\partial \mathbf{r}_k}{\partial \mathbf{x}_k}. \tag{14}$$

Then, using $\mathbf{r}_k := [\, x_1(k) \quad x_2(k) \quad i_k \,]^{\mathrm{T}}$ yields

$$\frac{\partial \mathbf{r}_k}{\partial \mathbf{x}_k} = \begin{pmatrix} 1 & 0 \\ 0 & 1 \\ 0 & 0 \end{pmatrix}. \tag{15}$$

Moreover, assuming that $\varphi(\cdot)$ is a Gaussian function as in (3), it gives

$$\frac{\partial \varphi\left(\|\mathbf{r}_k - \mathbf{t}_i\|\right)}{\partial \mathbf{r}_k} = -\frac{2}{\sigma_i^2} \varphi\left(\|\mathbf{r}_k - \mathbf{t}_i\|\right) (\mathbf{r}_k - \mathbf{t}_i). \tag{16}$$

Substituting (14)–(16) into (13) yields

$$\frac{\partial F(\mathbf{r}_k)}{\partial \mathbf{x}_k} = -\frac{2}{\sigma_i^2} \sum_{i=1}^{M} w_i \varphi\left(\|\mathbf{r}_k - \mathbf{t}_i\|\right) (\mathbf{r}_k - \mathbf{t}_i)^{\mathrm{T}} \frac{\partial \mathbf{r}_k}{\partial \mathbf{x}_k}. \tag{17}$$

IV. Implementation and Experimental Setup

The proposed SOC estimator is tested on a Li-Ion battery. Fig. 2 shows the general structure of the experimental setup. The hardware consists of a special interface circuit for sampling current, voltage, and battery temperature. The sampled data are transferred to a computer via the serial port. The programming language for data manipulation and processing is Visual C++. In addition, for acquiring data for training the RBF NN and for testing the proposed SOC estimator, a battery charger has been included that controls the on–off time of charging and discharging the battery. The charging technique is based on the reflex charging method, which is considered as one of the most effective charging schemes [44]. In this charging method, the battery is first charged with a constant current for a small period of time, followed by discharging for a very short time and a relax interval at the end. The entire charging process can be viewed on the computer monitor (Fig. 2).

Figs. 3–5 show the designed circuits for the sampling interface, the signal conditioning, and the controllable charger, respectively. As shown in Fig. 3, microcontroller 89C52 is used to transfer the sampled voltage, current, and temperature of the battery to the computer. Moreover, based on the given commands by the computer, this microcontroller controls the on–off time of charging and discharging by applying the appropriate inputs to the driver. For the temperature sensing, an LM35 sensor is used. This sensor is calibrated in kelvin and has a scale factor equal to 10 mV/°C. The entire experimental setup of the proposed method is carried out at room temperature. Hence, variations of the battery temperature play a negligible role in the charging/discharging process [45]. The temperature is shown here only for monitoring purposes. For the current sensing, since the maximum current of the charger is set to about 1.5 A, a 0.1- Ω 5-W resistor is used. Moreover, for voltage sensing, a differential amplifier is employed. For data sampling, the ADC0809 is used. This chip has a resolution of 8 bits and can convert analog inputs to discrete outputs in less than 50 μs. For sampling, the analog input in all eight channels must be in the range of 0–5 V. Hence, it is necessary to use a signal adaptor to match the sensors outputs with the analog inputs of ADC0809 through the signal conditioning circuits (Fig. 4).

Fig. 5 shows the controllable charger, designed for data acquisition as well as for testing the proposed technique for the SOC estimation. The charger consists of a current source and a discharging 3.9-Ω/5-W resistor as the load. These two circuits are controlled by the SW1 and SW2 inputs, respectively. Since Li-Ion batteries are very sensitive to voltages above their nominal voltages, a voltage regulator is designed to maintain the battery terminal voltage at 4.2 V. This voltage regulator consists of Q6, Q7, OP07, and LM317 (Fig. 5).

A. Battery SOC Estimation

As it was mentioned in Section II, the battery is modeled using an RBF NN, which is trained using the data obtained from the battery. Since the SOC of the battery is one of the inputs to the NN, it is necessary to measure the SOC using one of the available methods. For this reason, the ampere–hour counting technique, given in (2), is employed for collecting the training data. For calculating η_i, the energy delivered by the battery during discharging is divided by the rated energy (the nominal capacity) of the battery C_n. The sampling period Δt is equal to 0.8 s for the SOC estimation. It should be mentioned that the sampling rate of the experimental setup is

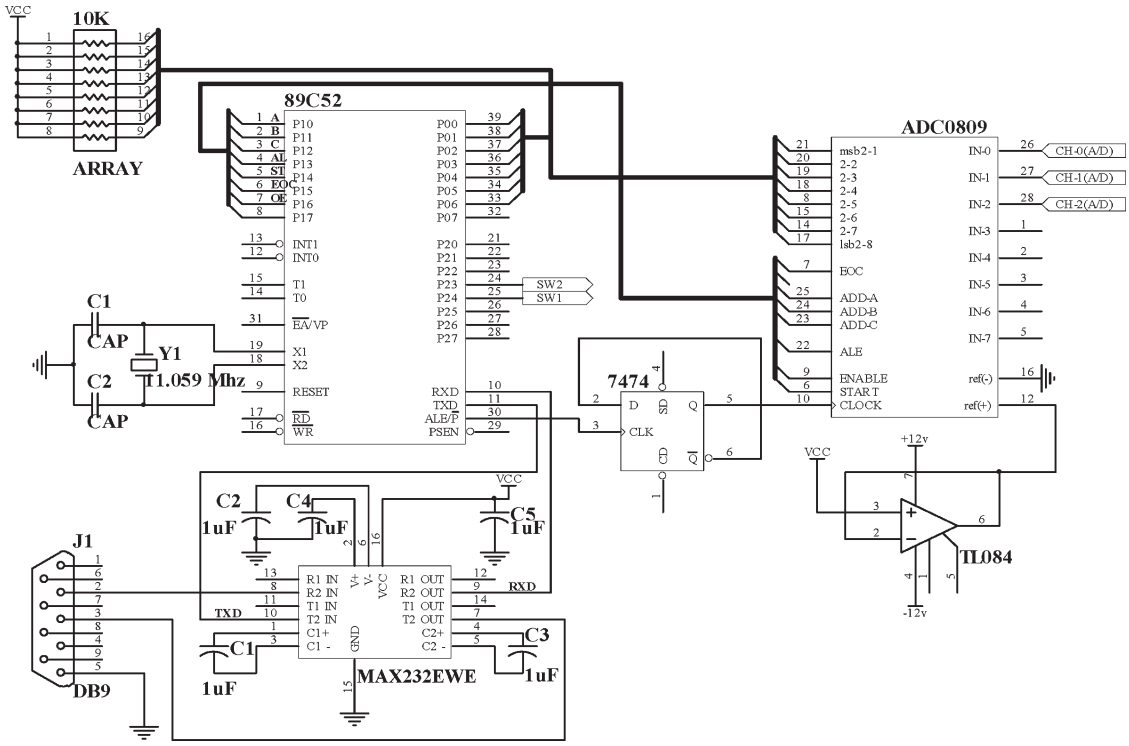

Fig. 3. Interfacing and sampling circuits.

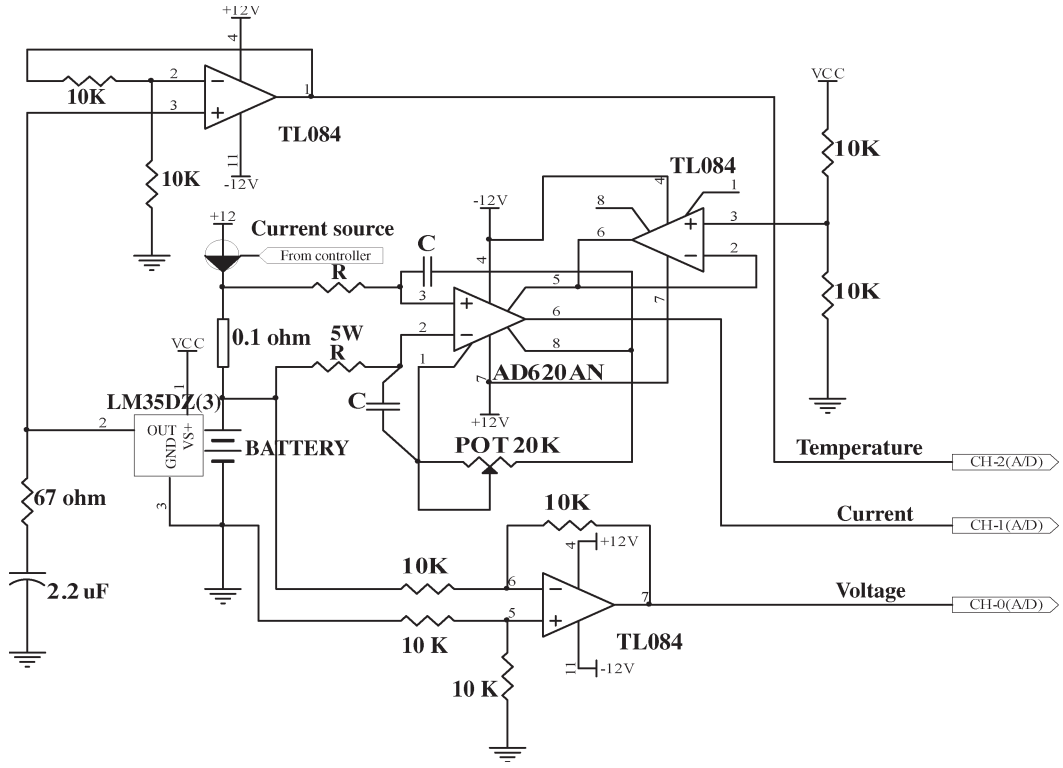

Fig. 4. Signal conditioning circuit.

50 ms, which is used for display purposes, but the SOC estimation process is updated every 800 ms.

Fig. 6 shows the data acquired from the experimental test on a 1.2-Ah Li-Ion battery. These data are used for the training of the RBF NN. Although the battery temperature is measured and saved here, it is not used for the estimation or charging processes; the experiments have been carried out at room temperature.

The covariance matrix $\mathbf{R}$ is determined from the data in Fig. 6 based on the mean of the square of the rms noise of the

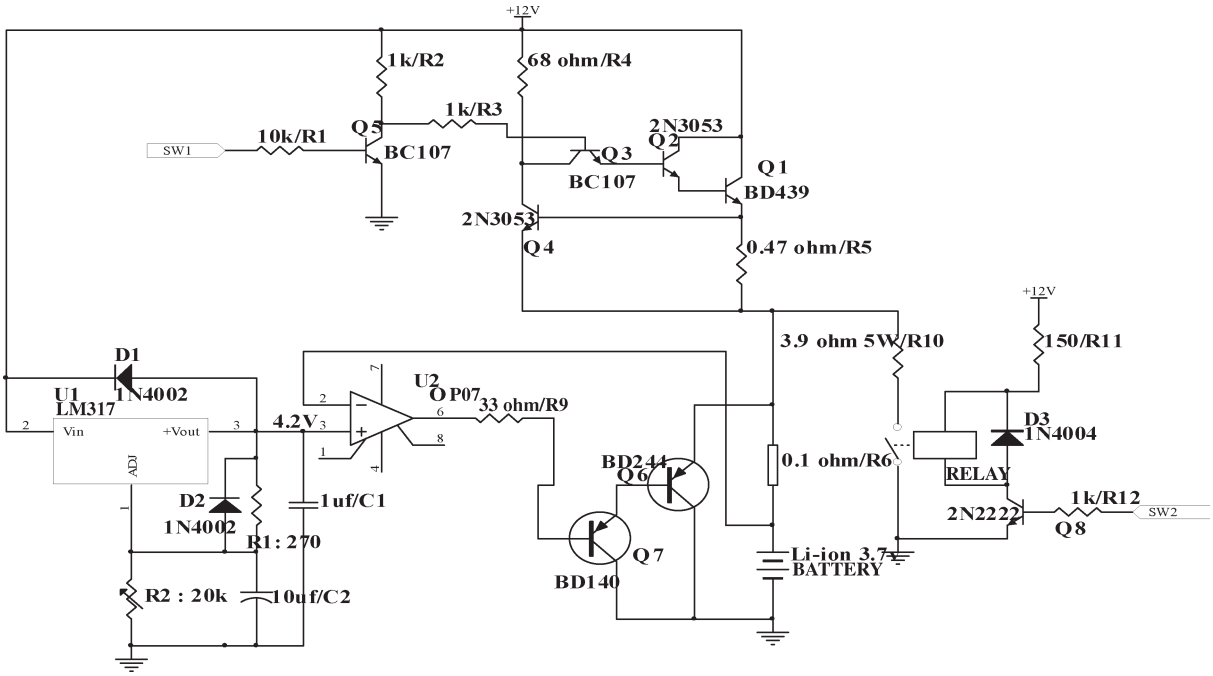

Fig. 5. Controllable charger circuit (driver) with voltage limiter.

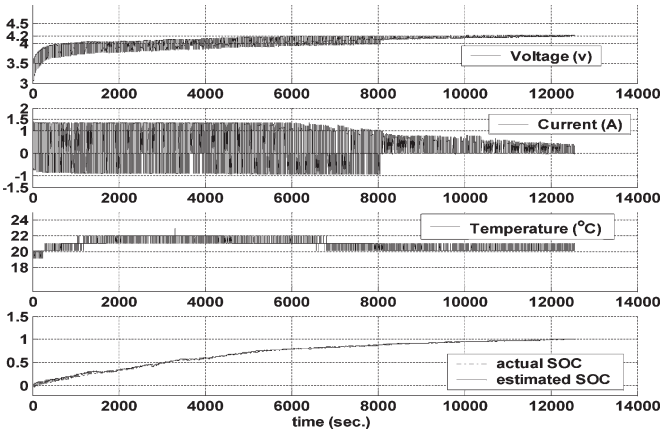

Fig. 6. Experimental data obtained from a full charging cycle of a 1.2-Ah Li-ion battery.

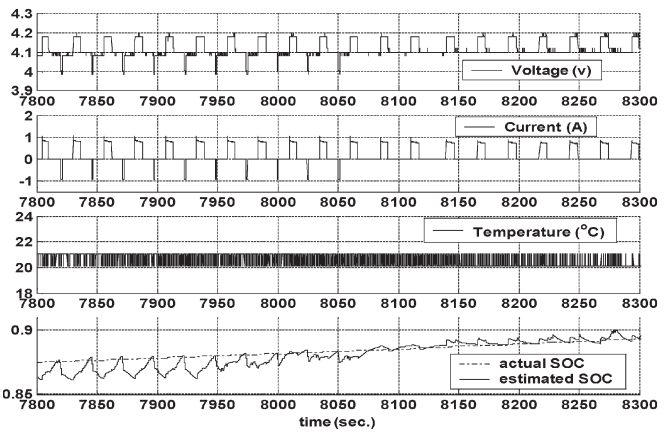

Fig. 7. 500 s of Fig. 6.

battery terminal voltage in the intervals of the charging process, where the amplitude of the charging current is constant. The calculated $\mathbf{R}$ is equal to $\mathrm{diag}[\,0.01 \quad 0.01\,]$.

The covariance matrix $\mathbf{Q}$ is determined adaptively using (9). The initial value of this matrix is set to $\mathrm{diag}[\,0.005 \quad 0.005\,]$. The variable N in (9) is selected equal to five. It is important to mention that the proposed algorithm is not very sensitive to the initial value of matrix $\mathbf{Q}$ and the parameter N. This is mainly due to the fact that matrix $\mathbf{Q}$ is adaptively adjusted to cope with the changes. Fig. 7 shows 500 s of Fig. 6 for better visualization.

Since the NN needs to be trained with different charging conditions, the entire charging cycle is divided into three parts: The first part is performed with 70% duty cycle, the second part is carried out with 35% duty cycle, and the third part is performed with 20% duty cycle.

In order to avoid overtraining of the NN, 3600 samples are selected out of every 240 000 samples (i.e., 3 samples out of every 200 samples). The inputs to the NN are $v(k-1)$, $i(k)$, and $SOC(k)$, while the output is the battery terminal voltage at the present sample $v(k)$. These variables are normalized based on their maximum values. There are 30 neurons in the hidden layer with $\sigma_i = 1.0\ (i = 1, \ldots, 30)$. These numbers are usually defined with trial and error [38]. At the end of the training phase, the rms error for all 3600 samples is almost 0.17 (i.e., almost 4%).

Next, the trained NN is used as a model in the EKF to estimate the same SOC shown in Fig. 6. The block diagram of the estimation algorithm is shown in Fig. 8. The result of the SOC estimation is shown in Fig. 9. The rms error (between the actual SOC and the estimated one) is equal to 2%, which can be considered as a good accuracy. Fig. 10 shows how the elements of the estimated covariance matrix for the system noise are varying during the SOC estimation.

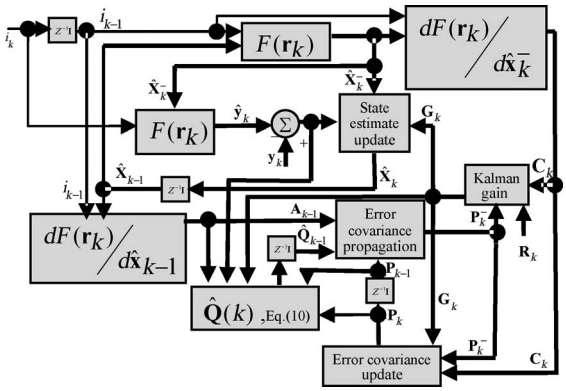

Fig. 8. Block diagram of the implemented estimation algorithms.

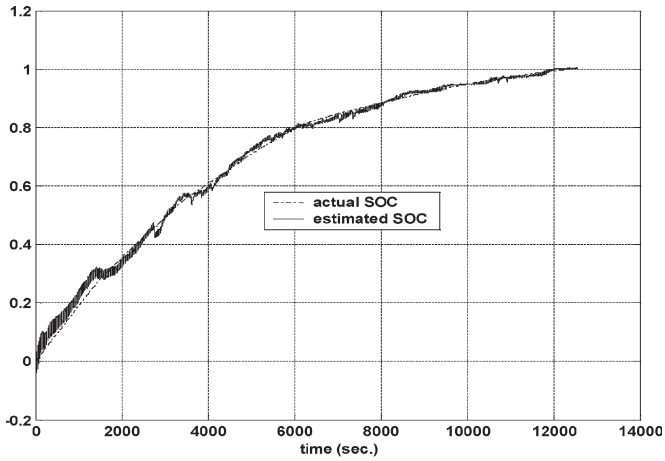

Fig. 9. (Dashed line) Desired SOC measured by the ampere–hour counting technique and (solid line) the estimated SOC using the EKF and the NN.

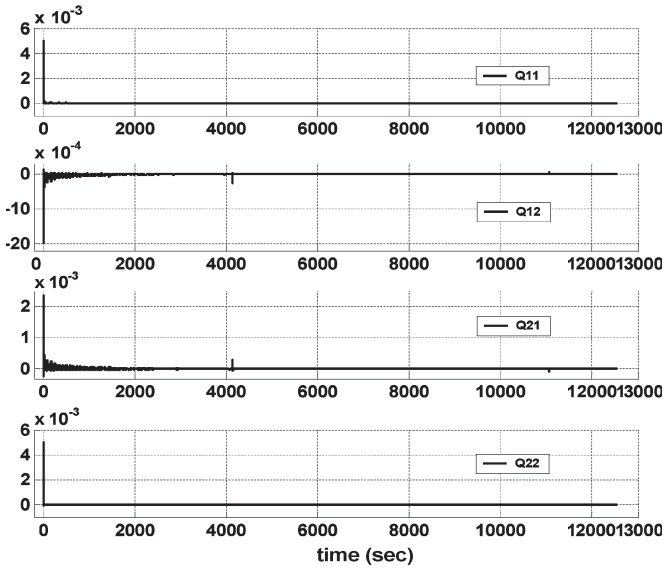

Fig. 10. Variations in the system noise covariance matrix $\mathbf{Q}$ using the adaptive procedure.

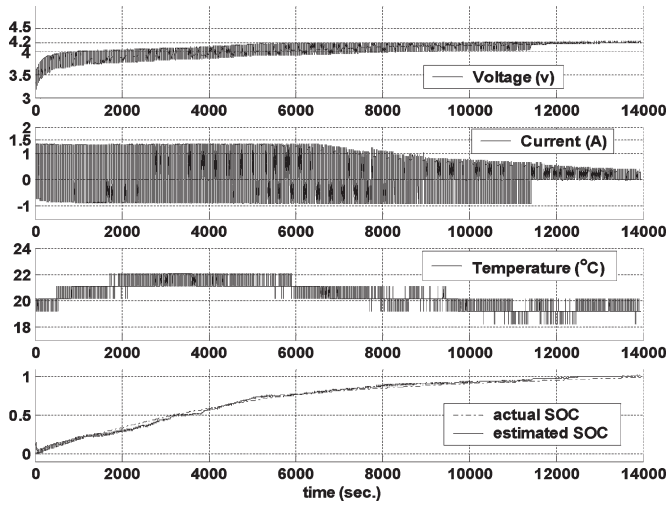

Fig. 11. Controlled battery charging using the proposed estimator.

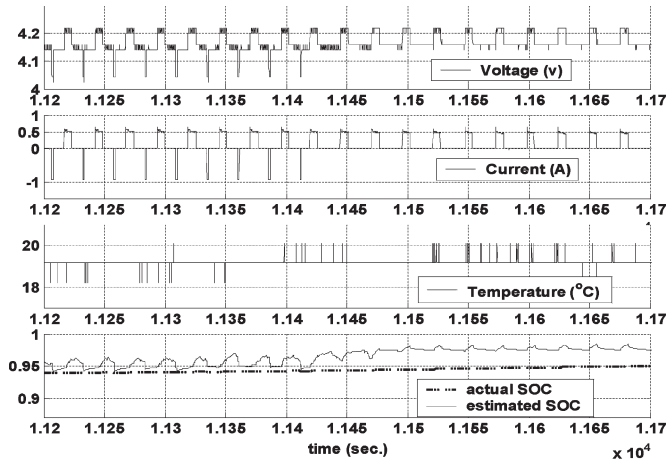

Fig. 12. 500 s of Fig. 11.

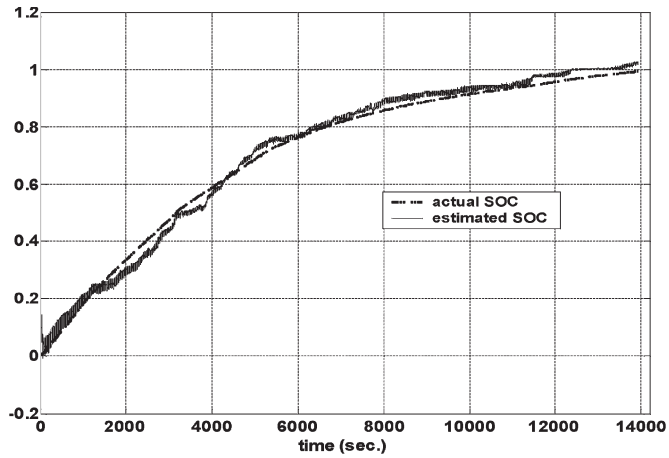

Fig. 13. Actual and the estimated SOC during charging process, using the proposed estimator.

B. Experimental Tests

Up to this point, the training and testing of the RBF NN along with the adaptive EKF are performed offline. Next, the designed SOC estimator is tested in the controlled and online charging processes for the same Li-Ion battery. The results are shown in Figs. 11–14. Fig. 11 shows the battery terminal voltage, the charging current, the battery temperature, and the actual SOC waveforms. For clarity, 500 s of Fig. 11 is shown in Fig. 12.

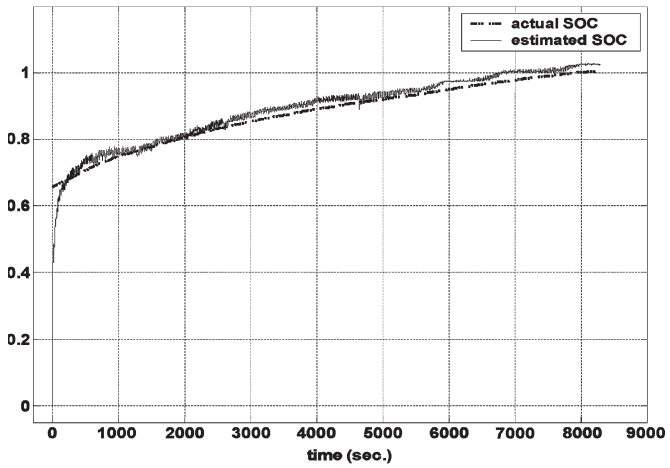

Fig. 14. Testing the proposed SOC estimator with different initial conditions for state variables of EKF (disconnecting the power supply for 30 min).

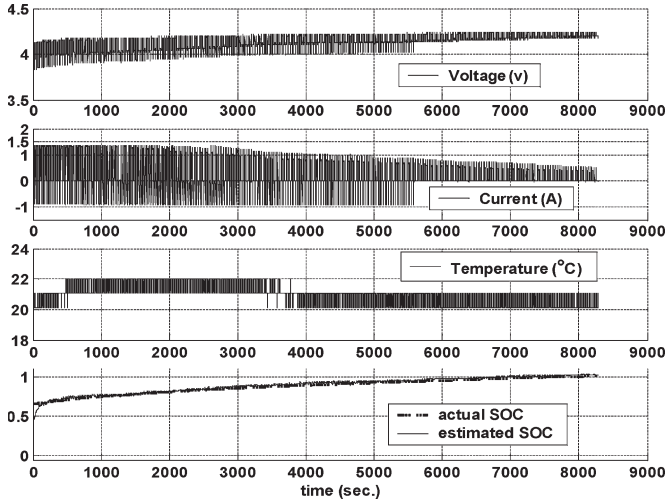

Fig. 15. Controlled battery charging using the proposed estimator.

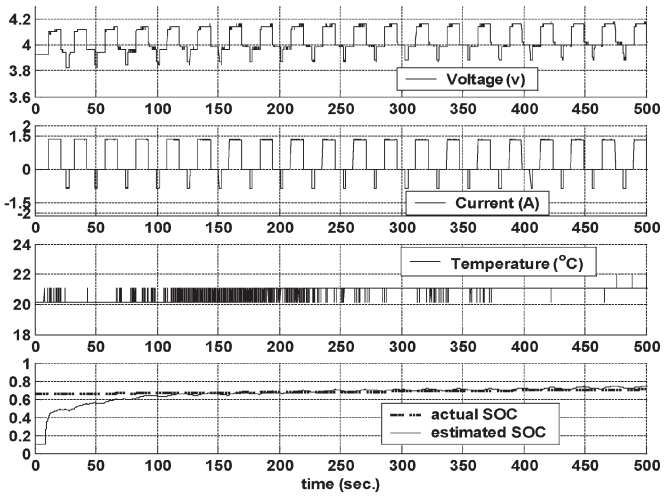

Fig. 16. First 500 s of Fig. 15.

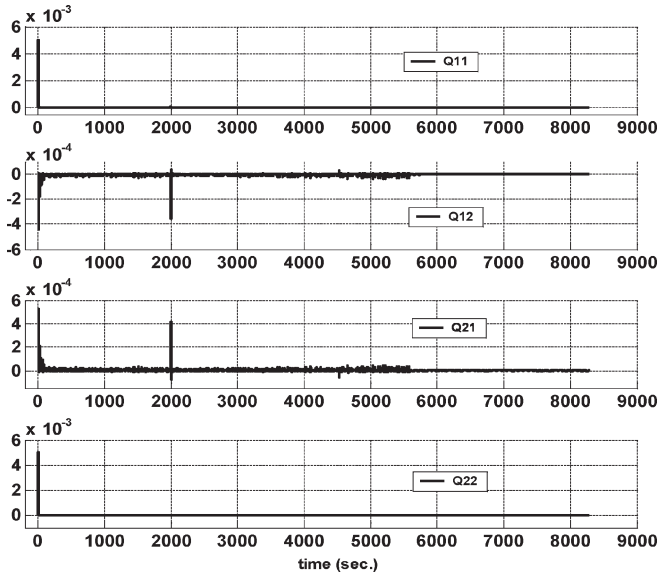

Fig. 17. Variations in the system noise covariance matrix $\mathbf{Q}$ using the adaptive procedure.

Fig. 13 shows the actual and the estimated SOCs during the entire charging process. The rms error (between the actual SOC and the estimated SOC) is almost 3%. As shown in Fig. 11, at the beginning of the charging process, the reflex charging method has been used followed by the pulse charging technique (at about $SOC = 90\%$), in which the negative pulses have been eliminated for the remaining of the charging period.

Next, for testing the designed estimator with different initial conditions of the state variables, the battery is charged to about 65% of its nominal capacity. Then, it is separated from the charger, and the charger is disconnected from the power supply for about 30 min. Then, the battery-charging process is resumed using the same initial conditions as if the battery were empty. The test results are shown in Figs. 14–17. As it is clear from Fig. 14, the estimated SOC converges quickly to the actual SOC in less than 2.5 min, which shows that the proposed estimator is robust against different initial conditions. The rms error is almost 3% for this case. Figs. 15 and 16 show the battery terminal voltage, the charging current, the battery temperature, and the actual and the estimated SOC waveforms. Finally, Fig. 17 shows variations in elements of the covariance matrix $\mathbf{Q}$.

Variations in Q21 at the beginnings are indications of the quick reaction of the EKF to converge the actual SOC. As it was mentioned before, whenever the eigenvalues of matrix $\mathbf{Q}$ become negative, they are set equal to zero [43].

V. Conclusion and Discussions

A SOC estimator for Li-Ion batteries using ANNs and EKF with adaptive covariance matrix for the system noise was proposed in this paper. The NN is of RBF type and was trained offline to find the appropriate model needed in the EKF, which estimates the SOC of the battery. The experimental results of the proposed estimator showed good accuracy and fast convergence to the actual state variables, independent of the charging conditions and/or initialization of the EKF. It should be noted that, since the input and output variables used for the NN are normalized, the proposed method could be used for a wide variety of rechargeable batteries. However, a few issues

about the proposed method need to be discussed here. These issues can give directions to the future works.

1) In order to apply the proposed method to a battery pack composed of many cells of the same type connected in parallel and series, it is necessary to measure the current and voltage of each cell. Consequently, the SOC is calculated for each cell separately using the same model.
2) The proposed method was carried out in room temperature. However, batteries are used in different environmental conditions and ambient temperatures. The simplest way to incorporate the battery thermal effect into the proposed method is to create a lookup table composed of different models [35]. In other words, the parameters of the proposed method are to be identified for each predefined temperature (e.g., over the temperature range of 5 °C–45 °C in the increment of 2 °C). This requires more memory for data storage and processing.
3) The data for training the NN were collected from a brand new and healthy battery. Hence, the trained NN may not yield acceptable output when the battery ages. This problem can be resolved using data gathered throughout the lifetime of the battery.

REFERENCES

[1] T. R. Crompton, *Battery Reference Book*, 3rd ed. Oxford, U.K.: Newnes, 2000.

[2] V. Pop, H. J. Bergveld, P. H. L. Notten, and P. P. L. Regtien, "State-of-the-art of battery state-of-charge determination," *Meas. Sci. Technol.*, vol. 16, no. 12, pp. R93–R110, Dec. 2005.

[3] S. Piller, M. Perrin, and A. Jossen, "Methods for state-of-charge determination and their applications," *J. Power Sources*, vol. 96, no. 1, pp. 113–120, Jun. 2001.

[4] J. Chatzakis, K. Kalaitzakis, N. C. Voulgaris, and S. N. Manias, "Designing a new generalized battery management system," *IEEE Trans. Ind. Electron.*, vol. 50, no. 5, pp. 990–999, Oct. 2003.

[5] C. S. Moo, K. S. Ng, and Y. C. Hsieh, "Parallel operation of battery power modules," *IEEE Trans. Energy Convers.*, vol. 23, no. 2, pp. 701–707, Jun. 2008.

[6] S. M. Lukic, J. Cao, R. C. Bansal, F. Rodriguez, and A. Emadi, "Energy storage systems for automotive applications," *IEEE Trans. Ind. Electron.*, vol. 55, no. 6, pp. 2258–2267, Jun. 2008.

[7] H.-S. Park, C.-E. Kim, C.-H. Kim, G.-W. Moon, and J.-H. Lee, "A modularized charge equalizer for an HEV lithium-ion battery string," *IEEE Trans. Ind. Electron.*, vol. 56, no. 5, pp. 1464–1476, May 2009.

[8] E. Meissner and G. Richter, "Vehicle electric power systems are under change: Implications for design, monitoring and management of automotive batteries," *J. Power Sources*, vol. 95, no. 12, pp. 13–23, Mar. 2001.

[9] P. J. Blood and S. Sotiropoulos, "An electrochemical technique for state of charge (SOC) probing of positive lead-acid battery plates," *J. Power Sources*, vol. 110, no. 1, pp. 96–106, Jul. 2002.

[10] G. C. Hsieh, L. R. Chen, and K. S. Huang, "Fuzzy-controlled li-ion battery charge system with active state-of-charge controller," *IEEE Trans. Ind. Electron.*, vol. 48, no. 3, pp. 585–593, Jun. 2001.

[11] A. H. Anbuky and P. E. Pascoe, "VRLA battery state-of-charge estimation in telecommunication power systems," *IEEE Trans. Ind. Electron.*, vol. 47, no. 3, pp. 565–573, Jun. 2000.

[12] O. Gerard, J. N. Patillon, and F. d'Alche-Buc, "Neural network adaptive modelling of battery discharge behavior," in *Lecture Notes in Computer Science*. Berlin, Germany: Springer-Verlag, 1997, pp. 1095–1100.

[13] F. Huet, "A review of impedance measurements for determination of state-of-charge or state-of-health of secondary batteries," *J. Power Sources*, vol. 70, no. 1, pp. 59–69, Jan. 1998.

[14] S. Rodrigues, N. Munichandraiah, and A. K. Shukla, "A review of state-of-charge indication of batteries by means of ac impedance measurements," *J. Power Sources*, vol. 87, no. 1/2, pp. 12–20, Apr. 2000.

[15] L. R. Chen, "A design of an optimal battery pulse charge system by frequency-varied technique," *IEEE Trans. Ind. Electron.*, vol. 54, no. 1, pp. 398–405, Feb. 2007.

[16] M. Coleman, C. K. Lee, C. Zhu, and W. G. Hurley, "State-of-charge determination from EMF voltage estimation: Using impedance, terminal voltage, and current for lead-acid and lithium-ion batteries," *IEEE Trans. Ind. Electron.*, vol. 54, no. 5, pp. 2550–2557, Oct. 2007.

[17] A. J. Salkind, C. Fennie, P. Singh, T. Atwater, and D. E. Reisner, "Determination of state-of-charge and state-of-health of batteries by fuzzy logic methodology," *J. Power Sources*, vol. 80, no. 1/2, pp. 293–300, Jul. 1999.

[18] P. Singh, C. Fennie, and D. E. Reisner, "Fuzzy logic modeling of state-of-charge and available capacity of nickel/metal hydride batteries," *J. Power Sources*, vol. 136, no. 2, pp. 322–333, Oct. 2004.

[19] K. Kutluay, Y. Çadýrcý, Y. S. Özkazanç, and I. Çadýrcý, "A new online state-of-charge estimation and monitoring system for sealed lead-acid batteries in telecommunication power supplies," *IEEE Trans. Ind. Electron.*, vol. 52, no. 5, pp. 1315–1327, Oct. 2005.

[20] T. Yamazaki, K. Sakurai, and K. I. Muramoto, "Estimation of the recharge capacity of sealed lead-acid batteries by neural network," in *Proc. IEEE ITEC*, San Francisco, CA, 1998, pp. 210–214.

[21] J. Peng, Y. Chen, and R. Eberhart, "Battery pack state of charge estimator design using computational intelligence approaches," in *Proc. IEEE ABAC*, Long Beach, CA, 2000, pp. 173–177.

[22] S. Grewal and D. A. Grant, "A novel technique for modeling the state of charge of lithium ion batteries using artificial neural networks," in *Proc. IEEE ITEC*, 2001, pp. 174–179.

[23] C. H. Cal, D. Du, Z. Y. Liu, and H. Zhang, "Artificial neural network in estimation of battery state-of-charge (SOC) with nonconventional input variables selected by correlation analysis," in *Proc. IEEE MLC*, Beijing, China, 2002, pp. 1619–1625.

[24] C. Cai, D. Du, Z. Liu, and J. Ge, "State-of-charge (SOC) estimation of high power NI-MH rechargeable battery with artificial neural network," in *Proc. IEEE NIP*, Singapore, 2002, pp. 824–828.

[25] C. H. Cai, D. Du, and Z. Y. Liu, "Battery state-of-charge (SOC) estimation using adaptive neuro-fuzzy inference system (ANFIS)," in *Proc. IEEE ICFS*, St. Louis, MO, 2003, pp. 1068–1073.

[26] W. X. Shen, C. C. Chan, E. W. C. Lo, and K. T. Chau, "Adaptive neuro-fuzzy modeling of battery residual capacity for electric vehicles," *IEEE Trans. Ind. Electron.*, vol. 49, no. 3, pp. 677–684, Jun. 2002.

[27] A. Affanni, A. Bellini, C. Concari, G. Franceschini, E. Lorenzani, and C. Tassoni, "EV battery state of charge: Neural network based estimation," in *Proc. IEEE ICEMD*, 2003, vol. 2, pp. 684–688.

[28] Y.-S. Lee, W.-Y. Wang, and T.-Y. Kuo, "Soft computing for battery state-of-charge (BSOC) estimation in battery string systems," *IEEE Trans. Ind. Electron.*, vol. 55, no. 1, pp. 229–239, Jan. 2008.

[29] S. Pang, J. Farrell, J. Du, and M. Barth, "Battery state-of-charge estimation," in *Proc. ACC*, Arlington, MA, 2001, pp. 1644–1649.

[30] B. S. Bhangu, P. Bentley, D. A. Stone, and C. M. Bingham, "Nonlinear observers for predicting state-of-charge and state-of-health of lead-acid batteries for hybrid-electric vehicles," *IEEE Trans. Veh. Technol.*, vol. 54, no. 3, pp. 783–794, 2005.

[31] A. Vasebi, S. M. T. Bathaee, and M. Partovibakhsh, "Predicting state of charge of lead-acid batteries for hybrid electric vehicles by extended Kalman filter," *Energy Convers. Manage.*, vol. 49, no. 1, pp. 75–82, Jan. 2008.

[32] O. Barbarisi, F. Vasca, and L. Glielmo, "State of charge Kalman filter estimator for automotive batteries," *Control Eng. Pract.*, vol. 14, no. 3, pp. 267–275, Mar. 2006.

[33] J. Lee, O. Nam, and B. H. Cho, "Li-ion battery SOC estimation method based on the reduced order extended Kalman filtering," *J. Power Sources*, vol. 174, no. 1, pp. 9–15, Nov. 2007.

[34] S. Santhanagopalan and R. E. White, "Online estimation of the state of charge of a lithium ion cell," *J. Power Sources*, vol. 161, no. 2, pp. 1346–1355, Oct. 2006.

[35] G. L. Plett, "Extended Kalman filtering for battery management systems of LiPB-based HEV battery packs, Part 2: Modeling and identification," *J. Power Sources*, vol. 134, no. 2, pp. 262–276, Aug. 2004.

[36] G. L. Plett, "Extended Kalman filtering for battery management systems of LiPB-based HEV battery packs, Part 3: State and parameter estimation," *J. Power Sources*, vol. 134, no. 2, pp. 277–292, Aug. 2004.

[37] G. L. Plett, "Kalman-filter SOC estimation for LiPB HEV cells," in *Proc. 19th Int. Battery, Hybrid Fuel Cell Electr. Veh. Symp. Exhib.*, Bousan, Korea, 2002, pp. 1–12.

[38] S. Haykin, *Neural Networks: A Comprehensive Foundation*, 2nd ed. Englewood Cliffs, NJ: Prentice-Hall, 1999.

[39] S. Haykin, *Kalman Filtering and Neural Networks*. New York: Wiley/Interscience, 2001.

[40] P. S. Maybeck, *Stochastic Models, Estimation, and Control*. New York: Academic, 1982.

[41] T. Kailath, "An innovations control approach to least square estimation. Part I: Linear filtering in additive white noise," *IEEE Trans. Autom. Control*, vol. AC-13, no. 6, pp. 646–655, Dec. 1968.
[42] K. A. Myers and B. D. Tapley, "Adaptive sequential estimation with unknown noise statistics," *IEEE Trans. Autom. Control*, vol. AC-21, no. 4, pp. 520–523, Aug. 1976.
[43] I. Blanchet, C. Frankignoul, and M. A. Cane, "A comparison of adaptive Kalman filters for tropical pacific ocean model," *Mon. Weather Rev.*, vol. 125, no. 1, pp. 40–58, Jan. 1997.
[44] C. C. Hua and M. Y. Lin, "A study of charging control of lead-acid battery for electric vehicles," in *Proc. IEEE ISIE*, Puebla, Mexico, 2000, vol. 1, pp. 135–140.
[45] A. A. Pesaran and M. Keyser, "Thermal characteristics of selected EV and HEV batteries," in *Proc. IEEE ABAC*, Long Beach, CA, 2001, pp. 219–225.

Mohammad Charkhgard was born in Karaj, Iran, in 1980. He received the B.S. degree in electronic engineering from Azad University, Tehran, Iran, in 2003 and the M.S. degree in control engineering from Iran University of Science and Technology, Tehran, in 2006.

His research interests include identification, estimation, and electronic circuit design.

Mohammad Farrokhi (M'92) received the B.S. degree in electrical engineering from K. N. Toosi University, Tehran, Iran, in 1985 and the M.S. and Ph.D. degrees in electrical engineering from Syracuse University, Syracuse, NY, in 1989 and 1996, respectively.

In 1996, he joined Iran University of Science and Technology, where he is currently an Associate Professor of electrical engineering. His research interests include automatic control, fuzzy systems, and neural networks.